PAVING THE ROAD TO FLEX AND BIOMASS : THE LAND SURFACE CARBON CONSTELLATION STUDY

N.J. Rodríguez-Fernández[1], M. Barbier[1], J. Verrelst[2], H. Lindqvist[3], E. Bueechi[4], P. Reyes Muñoz[2], A. Mialon[1], M. Vreugdenhil[4], W. Dorigo[4], A. Bouvet[1], Y. Kerr[1], M. Vossbeck[5], T. Kaminski[5], M. Scholze[6]

[1] CESBIO (CNRS, CNES, Université de Toulouse, IRD, INRAE), Toulouse, France
[2] Universitat de Valencia, Valencia, Spain
[3] Finnish Meteorological Institute, Helsinki, Finland
[4] TU Wien, Vienna, Austria
[5] The Inversion Lab, Hamburg, Germany
[6] Lund University, Lund, Sweden

ABSTRACT

Remote sensing observations of variables related to vegetation at microwave and optical/infrared wavelengths are presented over three regions in Europe in the Iberian peninsula, northern Finland and central Europe. They include the instrumented sites of Las Majadas, Sodankylä and Reusel. The final goal is to better constrain land carbon cycle models using the complementarities of vegetation optical depth derived at different frequencies from active and passive instruments (related to vegetation water content and biomass) as well as optical data of the fraction of absorbed photosynthetically active radiation or solar induced fluorescence, closely linked to photosynthesis. The first results confirm this complementarity. For instance, time series of different variables exhibit positive correlations in some areas and negative correlations in other areas.

Index Terms— L-Band, Vegetation Optical Depth, Soil Moisture and Ocean Salinity satellite,

1. INTRODUCTION

In the context of climate change it is important to understand and quantify CO_2 sources and sinks both in the ocean and the land surface. However, there are large uncertainties in the quantification of the terrestrial carbon sinks due to uncertainties in the parameterisations and parameter values of terrestrial carbon models. Reducing these uncertainties is critical for reducing the spread in simulations of the global carbon cycle, and hence in climate change projections. The Land Surface Carbon Constellation (LCC) project [1], as part of ESA's Carbon Science Cluster, is designed to reduce these uncertainties using an integrated approach exploiting both observations (satellite and in situ) and modelling. Regarding the Earth observation data, the project aims at making a synergistic exploitation of the vegetation optical depth (VOD) estimated from active and passive microwave sensors at different waveleghts (providing information on the vegetation water content and on the above ground biomass) together with optical observations of vegetation-related variables including the Fraction of Absorbed Photosynthetically Active Radiation (FAPAR) and the Solar Induced Fluorescense (SIF), closely related to the photosynthetic activity. In this context, the LCC project is a precursor of the science that will be done with ESA's Biomass and FLEX missions. These data will be assimilated into the new community terrestrial ecosystem model D&B that is being developed within LCC based on the well-established DALEC [2] and BETHY [3] models in one region of boreal foreset in Northern Finland and another region of temperate savanna in the Iberian peninsula. The model development as well as the satellite data interpretation is supported by dedicated field campaigns at Sodankylä (Finland) and Las Majadas de Tietar (Spain). A third region around the agricultural instrumented site in Reusel (The Netherlands) will also be used, in particular to asses the remote sensing data. The three regions are shown in Figure 1.

In this contribution, some of the data sets compiled for the LCC project are discussed. Visible and near-infrared indices are sensitive to green components of the vegetation as they are related to the photosynthetically active parts of the vegetation as indicated by variables from widely used indices such as NDVI (Normalized Difference Vegetation Index), to FAPAR or the more innovative SIF. FAPAR quantifies the fraction of the solar radiation absorbed by living leaves for the photosynthetic activity while SIF represents an emission of energy emanating via a pathway for de-excitation that is competing with photosynthesis. These indices can be used as proxy for the Gross Primary Production (GPP) but they saturate quickly even for moderate biomass values (<80 Mg/ha). Liu et al. [4] showed that passive microwave (MW) VOD with frequencies higher than 6 GHz can be used to estimate AGB while
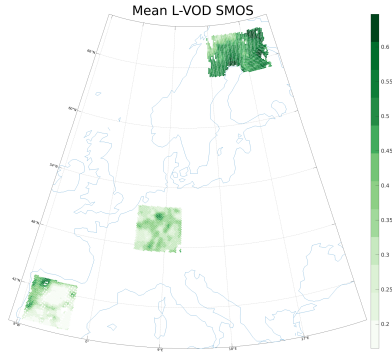
Fig. 1. Mean SMOS L-VOD in the period 2011-2020 in the three regions of the Land Surface Carbon Constellation study.
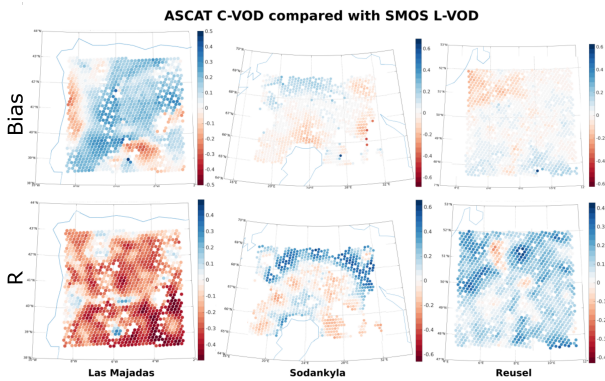

Fig. 2. The upper three panels show the bias of ASCAT VOD and SMOS L-VOD (mean of ASCAT VOD minus mean of SMOS VOD) for the three studied regions. The lower three panels show the Pearson correlation of SMOS and ASCAT VOD.

Rodriguez-Fernandez et al. [5] showed that passive L-band (1.4 GHz) VOD (L-VOD) is even more sensitive to AGB, without significant signs of saturation for high AGB values (300 – 400 Mg/h). Active and passive MW observations also give access to the hydrological state of the vegetation because VOD is directly related to the vegetation water content.

2. DATA

The data sets discussed in the current study are the following:

- Passive microwaves VOD obtained from different frequency bands: SMOS L-band VOD [6], AMSR-2 C1, C2 and X bands VOD [7]

- Active microwave VOD obtained with C-Band observations: ASCAT VOD [8]

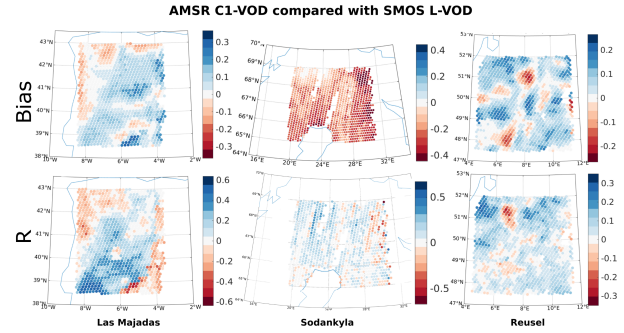- Sentinel 3 FAPAR [9]

- Sentinel 5P TROPOMI SIF [10]

Fig. 3. The upper three panels show the bias of ASMR-2 C1-band VOD and SMOS L-VOD (mean of AMSR-2 C1 VOD minus mean of SMOS VOD) for the three studied regions. The lower three panels show the Pearson correlation of SMOS and AMSR-2 C1-VOD.

- MODIS Enhanced Vegetation Index (EVI) and Normalized Difference Vegetation Index (NDVI)

The period of the present analysis is from 2010 to 2020, although some data sets do not span the full period.

3. RESULTS AND DISCUSSION

Figure 2 and Figure 3 show the bias and the Pearson correlation of SMOS L-VOD with respect to ASCAT C-VOD and AMSR-2 C1-VOD, respectively. The bias was computed as the mean of AMSR2 or ASCAT VOD minus the mean of SMOS VOD in the period 2011-2020. Equivalent figures were computed for comparing SMOS L-VOD with AMSR-2 C2 and X-bands VOD and they are very similar to those shown in Fig. 3.

ASCAT VOD shows an anticorrelation with respect to passive MW VOD (SMOS, shown in Fig. 2 but also with respect to AMSR2 VOD) in the Iberian peninsula. Correlations of ASCAT and SMOS VOD are also negative but with a low absolute value in many areas of the Finish region. Correlation maps show a low but positive correlation in Reusel (Fig. 2). The bias shows contrasted values in the three regions with areas showing positive values and areas with negative values in the three regions. Regarding AMSR2 and SMOS, the bias (AMSR2 - SMOS) is mainly positive in Las Majadas except in the north-western part of the region and also in Reusel. In contrast, it is negative in Sodankylä. Pearson correlations of ASMR-2 and SMOS VOD also show negative values in the north-west of Las Majadas, in the south-east of Sodankylä and in some regions of Reusel. The spatial distribution of the bias and the correlation maps were compared to land cover maps but no clear relationship has been found.

Figure 4 shows time series of AMSR2, SMOS and AS-CAT VOD in addition to SMOS soil moisture (SM), MODIS EVI and NDVI for the instrumented sites in the three regions.
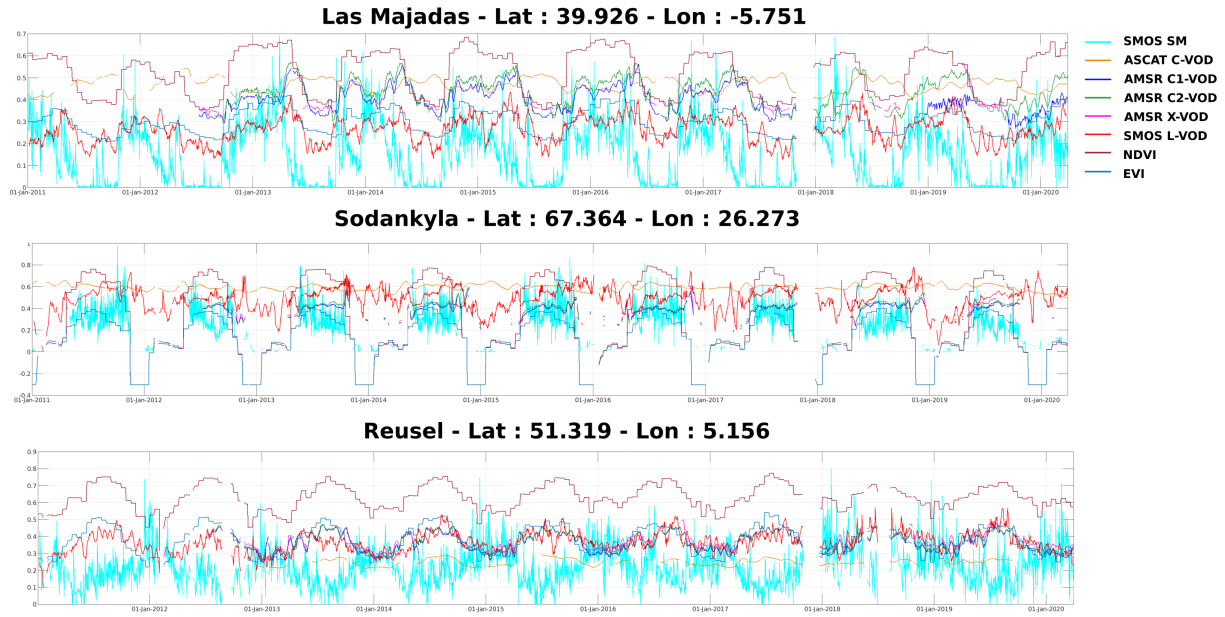
Fig. 4. Time series of SMOS L-VOD, AMSR2 C1, C2 and X-bands VOD, ASCAT C-VOD, MODIS NDVI and EVI at the closest grid point to the instrumented sites of Las Majadas, Sodankylä and Reusel.
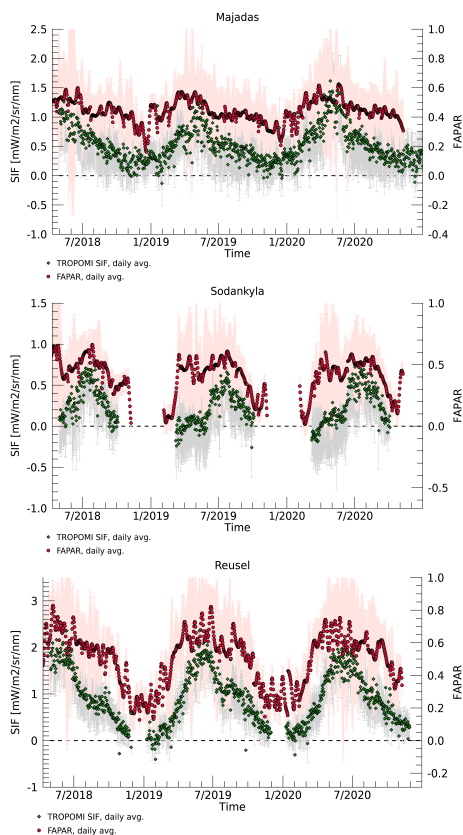

Fig. 5. Daily averages of TROPOMI SIF and Sentinel 3 FAPAR for the three sites.

Seasonal cycles of AMSR, SMOS VOD, NDVI and EVI are in good agreement in the three sites. However, the time series of the active MW ASCAT VOD is almost flat in Sodankylä and show an inverted cycle with respect to AMSR and SMOS VOD in Las Majadas. In Reusel ASCAT VOD is significantly lower than AMSR and SMOS VOD. Interestingly, the SMOS SM time series in Reusel shows a 180 days shifted cycle with respect to the vegeation related variables, both VOD and NDVI.

Depending on the frequency, MW radiation is sensitive to the water content in distinct parts of the vegetation, from the leaves, to the branches and the trunk (with small water-containing elements being transparent for long wavelength radiation). Assuming a relatively constant distribution of water molecules in the different parts of the plants/trees, the VOD should be higher for higher frequencies, which would suffer more absorption. However, ASCAT and AMSR2 VOD is lower than SMOS VOD in some areas. In addition, do the different seasonal cycles observed in the active and passive MW imply that the cycles of vegetation water content in different parts of the plants differ ? Definitely, more research is needed to understand the VOD data at different frequencies, ideally using homogenized VOD data sets.

Figure 5 shows time series of the daily average of Sentinel 5P SIF and Sentinel 3 FAPAR in the three instrumented sites. In Sodankylä, the correlation of SIF and FAPAR is 0.59, the lowest of all three sites. The time series shows an interesting detail in spring: FAPAR values peak already in March while SIF values are still close to zero. According to SIF, the start of photosynthesis occurs in late May or June. Despite their

different temporal changes in spring, both SIF and FAPAR start to decrease in August and appear coupled during the autumn. The reasons for these discrepancies can be speculated. First of all, evergreen boreal forests do not change reflectance according to seasons contrary to deciduous forests. In spring, the pine tree needles appear green although photosynthesis is not yet possible due to the frozen ground. The time series also includes the early and late winter months when SIF retrievals were not possible due to the limited amount of solar radiation and large solar zenith angles. The FAPAR estimates during these time periods may also be affected by these challenges and therefore appear unrealistic (e.g. the increase in FAPAR towards November may not be realistic). In spring, it may also be possible that a snow-covered surface induces biases in the FAPAR estimate, although bright pixels have been filtered in earlier data processing. In Las Majadas, the correlation of SIF and FAPAR is 0.71. The time series shows coupled variability at most seasons, except during late summer, FAPAR remains high although SIF decreases. This may be caused by limited water availability for photosynthesis which is seen in the decrease of SIF but, for the dominant vegetation type in the region, FAPAR may be a less sensitive indicator of drought. In Reusel, the correlation of SIF and FAPAR is 0.81, which is the highest of the three sites. The time series shows coupled variability at all seasons. An interesting detail is the double peak in SIF: the first and most significant maximum in June and another local maximum, although not as pronounced, in August-September. This appears also in FAPAR, although not as clearly. Possible reasons could be the land and crops management: e.g., harvest and irrigation.

4. CONCLUSIONS

Earth observation data concerning different variables related to vegetation were compared in the Iberian peninsula, northern Finland and the Netherlands. Different cycles were measured using VOD at several frequencies from active and passive microwave sensors. More research is needed to understand those cycles as well as the absolute values of VOD for all the frequencies. Optical data, although in overall good agreement, also show complementarities. The SIF data is particularly interesting as time series differ to those of other variables such as FAPAR at the beginning and the end of the growing season.

5. REFERENCES

[1] M. Scholze et al., "The land surface carbon constellation (LCC) project: Overview and first results," in *European Geophysical Union Symposium*, April 2022.

[2] Mathew Williams, Paul A Schwarz, Beverly E Law, James Irvine, and Meredith R Kurpius, "An improved analysis of forest carbon dynamics using data assimilation," *Global change biology*, vol. 11, no. 1, pp. 89–105, 2005.

[3] Wolfgang Knorr, "Annual and interannual CO2 exchanges of the terrestrial biosphere: Process-based simulations and uncertainties," *Global ecology and biogeography*, vol. 9, no. 3, pp. 225–252, 2000.

[4] Yi Y Liu, Albert I J M van Dijk, Richard a M de Jeu, Josep G Canadell, Matthew F McCabe, Jason P Evans, and Guojie Wang, "Recent reversal in loss of global terrestrial biomass: supplementary information," *Nature Climate Change*, vol. 5, no. May, pp. 1–5, 2015.

[5] Nemesio J Rodríguez-Fernández, Arnaud Mialon, Stephane Mermoz, Alexandre Bouvet, Philippe Richaume, Ahmad Al Bitar, Amen Al-Yaari, Martin Brandt, Thomas Kaminski, Thuy Le Toan, et al., "An evaluation of SMOS L-band vegetation optical depth (L-VOD) data sets: high sensitivity of L-VOD to above-ground biomass in Africa," *Biogeosciences*, vol. 15, no. 14, pp. 4627–4645, 2018.

[6] Y.H. Kerr, P. Waldteufel, P. Richaume, J.P. Wigneron, P. Ferrazzoli, A. Mahmoodi, A. Al Bitar, F. Cabot, C. Gruhier, S. Juglea, D. Leroux, A. Mialon, and S. Delwart, "The SMOS Soil Moisture Retrieval Algorithm," *IEEE Transactions on Geoscience and Remote Sensing*, vol. 50, pp. 1384–1403, May 2012.

[7] R. van der Schalie, R.A.M. de Jeu, Y.H. Kerr, J.P. Wigneron, N.J. Rodríguez-Fernández, A. Al-Yaari, R.M. Parinussa, S. Mecklenburg, and M. Drusch, "The merging of radiative transfer based surface soil moisture data from SMOS and AMSR-E," *Remote Sensing of Environment*, vol. 189, pp. 180–193, 2017.

[8] Mariette Vreugdenhil, Wouter A Dorigo, Wolfgang Wagner, Richard AM De Jeu, Sebastian Hahn, and Margreet JE Van Marle, "Analyzing the vegetation parameterization in the TU-Wien ASCAT soil moisture retrieval," *IEEE Transactions on Geoscience and Remote Sensing*, vol. 54, no. 6, pp. 3513–3531, 2016.

[9] P. Reyes Muñoz et al., "Mapping essential vegetation variables over europe using gaussian process regression and sentinel-3 data in Google Earth Engine," in *2021 IEEE International Geoscience and Remote Sensing Symposium IGARSS*, 2021, pp. 6260–6263.

[10] Luis Guanter, Cédric Bacour, Andreas Schneider, Ilse Aben, Tim A van Kempen, Fabienne Maignan, Christian Retscher, Philipp Köhler, Christian Frankenberg, Joanna Joiner, et al., "The TROPOSIF global sun-induced fluorescence dataset from the Sentinel-5P TROPOMI mission," *Earth System Science Data*, vol. 13, no. 11, pp. 5423–5440, 2021.